Canadian Mineralogist
Vol. 26, pp. 391-406 (1988)

SYMMETRY AND MORPHOLOGY OF SNOWFLAKES AND RELATED FORMS

CECIL J. SCHNEER
Department of Earth Sciences, University of New Hampshire, Durham, New Hampshire 03824, U.S.A.

ABSTRACT

Snowflakes, iodargyrite flakes, virus aggregates and AlMn alloys (called shechtmanite) are pattern invariant with transformations that are similarities, rather than congruences (self-similar scaling, *SSC*). Snowflakes, like fractals, are generated by recursive subdivision. *SSC* symmetry commutes with the point-group symmetry of ice to generate the hypersymmetric point group *6mm*:*SSC*. The structure of iodargyrite flakes observed at the micrometer scale is an eighth-order recursive hexagonal tiling of the atomic structure observed at the scale of the angstrom. The dense packing of spheres in a hierarchic succession of icosahedral shells (*ISP*) is related to a self-similar scaling of icosahedra (*B*) with symmetry *5m3*:*SSC* and the Fibonacci proportions, proposed for the structure of shechtmanite. Systematic development of permutations of the two hierarchic structures identifies one viral infection as a ninth-order icosahedral shell packing of *Herpes simplex* virions, each of which is itself a fourth-order icosahedral shell, ISP_9 (IS_4). The surface structure at the micrometer scale of *Adenovirus* is IS_5, *Tipula iridescens* IS_9; for *Papovavirion*, B_2; for *Parvovirion*, an incomplete B_2. Shechtmanite 'snowflakes' are *5m3*: *SSC* pentagonal tilings analogous to the *SSC*:*6mm* tiling of iodargyrite. Sections through the *B* model for shechtmanite illustrate the tiling symmetry. To the extent that these structures are fractal, fundamental physical and chemical parameters such as the length of the perimeter of the snowflake or its surface area, are indeterminate and ideal physical-chemical analysis is inapplicable.

Keywords: snowflake, iodargyrite, shechtmanite, self-similar scaling, Herpes simplex virion, crystal structure, tiling symmetry.

SOMMAIRE

Les flocons de neige et d'iodargyrite, les agrégats de virus et les alliages AlMn ("shechtmanite") possèdent une invariance dans leur morphologie, et leurs transformations dépendent de ressemblances, plutôt que de congruences (modification de l'échelle par similitude, encore notée en anglais: *SSC*). Les flocons de neige, tout comme les fractals, se propagent par subdivision successive. La symétrie *SSC*, ajoutée à l'élément de symétrie ponctuelle de la glace, donne le groupe ponctuel hypersymétrique *6mm*:*SSC*. La structure de cristaux d'iodargyrite, examinée à l'échelle micrométrique, comporte un agencement successif de huitième ordre de modules hexagonaux de la structure cristalline à l'échelle atomique. L'agencement dense de sphères dans une succession hiérarchique d'anneaux icosaédriques (*ISP*) est lié à une modification de l'échelle d'icosaèdres (*B*) ayant une symétrie *5m3*:*SSC* et les proportions de Fibonacci, telles que celles proposées pour la structure de la shechtmanite. Le développement systématique des permutations des deux structures hiérarchiques démontre qu'une des infections virales comporterait un agencement de neuvième ordre d'anneaux icosaédriques des virions *Herpes simplex*, chacun de ceux-ci étant un anneau icosaédrique de quatrième ordre, $ISP_9(IS_4)$. À l'échelle micrométrique, la structure de la surface de *Adenovirus* est IS_5, celle de *Tipula iridescens*, IS_9, celle de *Papovavirion*, B_2, et enfin celle de *Parvovirion*, B_2 incomplet. Les cristaux de "neige" de shechtmanite sont faits de modules pentagonaux *5m3*:*SSC* analogues aux modules *6mm*:*SSC* de l'iodargyrite. Des sections à travers le modèle *B* de la shechtmanite démontrent la symétrie des modules. Dans la mesure où il s'agit de structures fractales, les paramètres physiques et chimiques fondamentaux, tels que le périmètre d'un flocon ou l'aire de sa surface, sont indéterminés; c'est pourquoi une analyse physico-chimique idéale ne peut être appliquée.

(Traduit par la Rédaction)

Mots-clés: flocon de neige, iodargyrite, shechtmanite, modification de l'échelle par similitude, virion *Herpes simplex*, structure cristalline, symétrie des modules.

INTRODUCTION

The morphology of the variety of dendritic ice crystal commonly called *snowflake* can be described as the recursive subdivision of a generating pattern in such a way that each of its parts is a scaled replication of the original. This process, called self-similar scaling, is borrowed from fractal geometry. Although much of the detail of a snowflake and other dendrites is visible to the unaided eye or with an optical microscope, further detail, or even the existence of an ordered succession of distinguishable structures (a hierarchy) in other minerals and condensed materials, may require observation at the scale of the micrometer. Hierarchic structures may be overlooked because, like the snowflake, such materials appear to be classically crystalline by X-ray- or electron-diffraction analysis. For example, we have found a self-similar scaling of the basic hexagonal tiling of iodargyrite (AgI) in the "snowflake" habit possibly repeating over eight orders of hierarchic recursion (Fig. 1). Hierarchic structure seems to account for the pentagonal symmetry that,

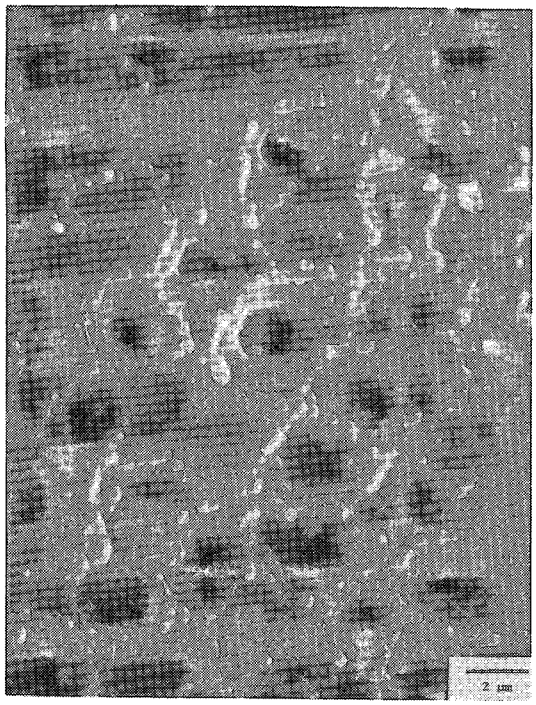

FIG. 1. Self-similar scaling of hexagonal nets of iodargyrite on a micrometer scale. Focused within the upper frond-like flake of Figure 10b southeast about halfway from the center to the edge. At 5000×, the structure consists of a successive sheeting of hexagonal nets, overlapping from northeast to southwest.

although incompatible with translation periodicity, has been observed in microclusters of gold (Komoda 1968) and minerals reported as fiveling twins (Palache 1932). We have traced the well-documented pentagonal symmetry of virus infections through several levels of structural organization where it appears to be combined with self-similar scaling. We find as well that the same operation of self-similar scaling commutes with pentagonal symmetry in the geometry of $Al_{\sim 6-12}Mn$ alloys, recently reported by Shechtman *et al.* (1984). The description of materials in this state of organization may require Mandelbrot's (1983) fractal dimension rather than the common concept of topological dimension. The properties and behavior of materials with such structure should reflect the discrepancy with classical views of crystallography and macrostructure. The density of the ordinary dendritic snowflake, for example, is not a thermodynamically intensive property constant within a defined boundary but decreases rapidly with distance from the center. Familiar geometric parameters, such as the length of the perimeter of the snowflake, are determined by the scale of the observation. Volume, area, stoichiometric proportions and, with them, physical quantities such as surface energy and mass, may require reassessment to fit these structures to the fractal geometry inherent in their symmetric expansion about a central point (dilational symmetry). At a micrometer scale the snowflake and the structurally related flakes of iodargyrite combine the symmetry of self-similar scaling (hereafter designated *SSC*) with the dihexagonal point-group symmetry of the macroscopic flake (designated *6mm* in the standard textbooks). The full symmetry, *6mm:SSC*, is expressed in Figure 2. At the atomic scale the same dihexagonal point symmetry combines with translation periodicity to form the space group of diffraction theory.

Two kinds of structural models have been proposed to account for the high-resolution diffraction patterns of melt-quenched AlMn 'microclusters' or 'quasicrystals' (Levine & Steinhardt 1984, Ogawa 1985, Hiraga *et al.* 1985). Both models combine self-similar scaling with the point-group symmetry of the regular icosahedron and dodecahedron: *5m3* in the notation of Mackay *et al.* (1977). Pentagonal symmetry is incompatible with translation periodicity at any scale so that the icosahedral point group *5m3* is not one of the 32 point groups of classical crystallography.

These examples have in common rates of formation that are extremely rapid as compared to ordinary rate of crystal growth. Although described as disequilibrium phases, it would seem that, to the extent that their dimensionality is fractal rather than topological, thermodynamic concepts such as phase, state or equilibrium (or combination thereof) are not directly applicable. Beyond the field of crystallography as presently defined (hence terms such as 'quasicrystals' and 'microcrystals'), these structures nevertheless may exhibit as high a degree of order as any known to material science.

DEFINITION OF SYMMETRY ELEMENTS

Crystallography has restricted its attention to congruent automorphisms, that is, to the special case of invariance with respect to scale. Of the congruent automorphisms which are rotations about a point, only rotations of $360/n$ with $n = 1,2,3, 4$ or 6 are considered crystallographic because these are the point-rotation symmetries compatible with congruent translation. Nevertheless, as Weyl (1952) has pointed out, for the general group of geometric automorphisms, "...the operation under which the pattern is invariant is not of necessity a congruence but could be a similarity." An indefinite iteration of a dilation from a fixed point at a definite scale is an operation of symmetry. Examples are spirals, such as in *Turritella* and the chambered nautilus. It is the pur-

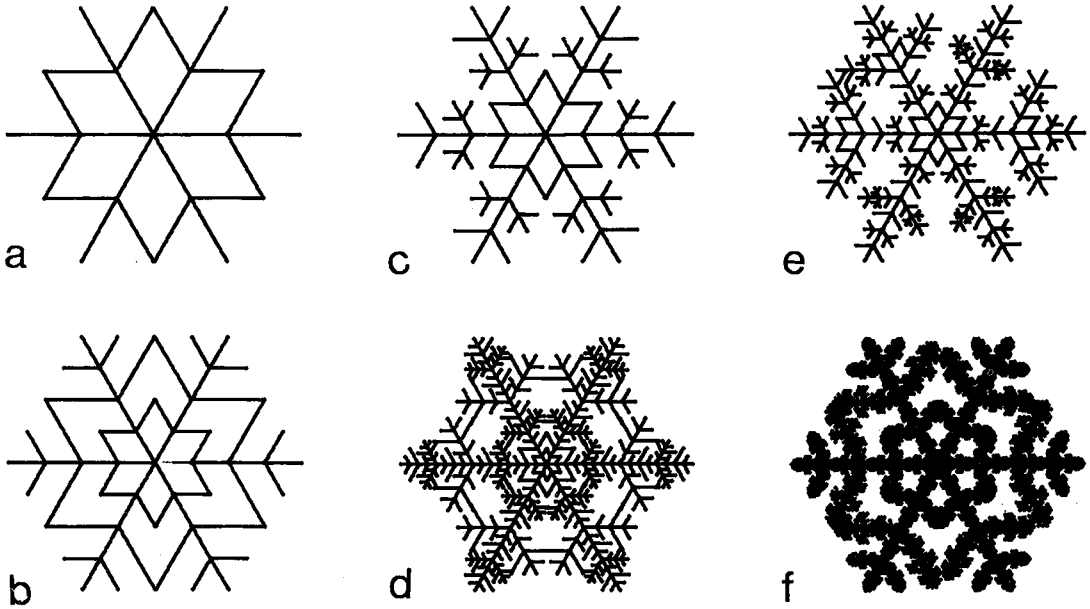

FIG. 2. Fractal models of snowflakes. (a) First order: a simple crowfoot of four equal segments (generator) is imposed upon each of the six arms of a hexagonal initiator. (b) First order: a compound crowfoot with generator pattern of 10 segments is imposed upon the same initiator. (c) Second order: the simple crowfoot generator is imposed upon each of the 6 × 4 segments of the first-order snowflake. The proportions of the arms (first order) were reduced. (d) Second order: the compound crowfoot generator pattern is imposed upon each of the 6 × 10 segments of the first order. (e) Third order: the simple generator pattern, with arm proportions randomized, is imposed upon each of the 96 segments of the second-order model (c). The randomization was undertaken to simulate the irregularities of natural habits. With randomization the scaling is statistical. (f) Third order: the compound generator with arm proportions randomized, is imposed upon each of the 600 segments of (d) above.

pose of this paper to propose dilational scaling self-similarity and the related phenomenon of hierarchic invariance as an additional class of symmetry operations useful for a more precise definition of morphology and structure in nature, and for the extension of our understanding of the order in natural materials.

SCALING SELF-SIMILARITY AS A RECURSIVE AUTOMORPHISM

Scaling self-similarity is defined by Mandelbrot (1983) as the recursive subdivision of a generating pattern so that each of its parts replicates the generator pattern to scale. A simple example is the cereal

FIG. 3. Generation of a third order fractal snowflake with exact scaling self-similarity. Compare these patterns with those of Bentley & Humphreys (1931, p.165 et passim). The proportions of the branch lengths in the largest order recursions determine the major features of the final snowflake.

box with the picture on it of the cereal box with the picture on it... *etc.* The first stage of the generator is imposed on an initial configuration (the initiator), as for example, a line segment or a triangle or a rhombohedron *etc.*, not necessarily similar to the generator. A model snowflake discussed below is constructed by successive recursions of a simple crowfoot generator on the six arms of the trigonal Miller–Bravais axes, a_1,a_2,a_3, as initiator (Schneer 1985, 1988).

We distinguish two kinds of scaling self-similarity; the first, that of the snowflake, the central point of which is unique and remains fixed throughout the symmetry operation, and a second, lacking a unique point as in a Penrose tiling or, in the trivial case of a scale of 1, an ordinary lattice. The first, or point symmetry, is dilational in that parameters such as density that are intensive in classically crystalline materials, in materials such as the snowflake, decrease with increasing distance from the point.

Consider the point-symmetry operation, dilational scaling self-similarity, *SSC* to be characterized by a generator G_p defined as a spatial configuration of elements I_{p-1} such that the configuration G_{p-1} for every element is the same (to a scale r) as G_p; p, the ordinal number of the recursion, is any integer. Such configurations are examples of Mandelbrot's *fractals* to the extent that ordinary dimensional measures of the configuration, such as the total number of cereal boxes, or the total length of the segments of one of the snowflakes illustrated in Figures 2 and 3, are indefinable. Scaling self-similarity is not necessarily fractal. The 2- and 3-dimensional Penrose tilings proposed as models for the shechtmanite structure are self-similar scaling (Levine & Steinhardt 1984, Ogawa 1985) but they are space-filling and dimensionally normal.

The highly symmetrical patterns of dendritic snow crystals (snowflakes) are reproducible by as few as 3 recursions of a simple linear motif (the generator *G*). The simplest of these motifs is the crowfoot peace symbol of the 60's, a line 2 units long, with two branches of unit length each at the midpoint deviating from the direction of the line by 60° on either side. In constructing algorithms for the representation of the snowflake models of the figures, the recursions were undertaken in either of two equivalent ways. We define the first algorithm as *synthetic* or dilational, in which identical units of the generator pattern are added at the scale of a lower cut-off limit, and the second as *analytic*, in which the initiator with the overall size of the final pattern is recursively divided into segments I_{p-1} by the motif of the generator G_p, (Fig. 2). In ideal synthetic growth, the crystal develops outward from a central point. In ideal analytic growth, material within a fixed volume condenses to an orderly pattern. The final form of real crystals might be reached by either, or by any combination of the two. For the computer-generated fractal models of the snowflake, each segment of the motif in turn bears the pattern at the scale of the next recursive stage. Complicating the pattern of the motif, as by adding more than 2 branches or altering the proportional lengths of the branches, or complicating the initiator, makes possible the replication of a very wide variety of natural snowflake patterns (Fig. 3).

The replication of many patterns found in snowflakes requires a difference or differences between the generator pattern for the largest recursion or recursions and that used for the others. The same total pattern may be achieved with analytic growth by appropriately complicating the initiator.

The ordinary topological dimensions, that is, length, area and volume, are functions of the recursive stage (hierarchic level). For the simple crowfoot as defined above, each recursion doubles the total length of all parts. If we were to start with the line [0,1] as initiator and continue by adding branches to convert it to a simple crowfoot, the length is effectively doubled to 2. Converting each of the three forward toes and the single backward toe to a crowfoot brings the total length to 4. Each recursion, adding branches scaled ½ the length of the segment to each of $N=4$ segments, doubles the total length again. For such a pattern, the topological concepts of surface (area) or bulk (volume) are consequences of the coarseness of the scale of observation. There is no unique value of length. There is no surface or volume in a rigorous sense, and therefore surface energy and bulk energy are not definable in ordinary terms.

Consider the density of the AgI "snowflakes" discussed below. The published density of iodargyrite (5.683 g/cm^3), like that of most materials, was calculated from the X-ray data (Swanson *et al.* 1959), that is, it was determined indirectly from observations made at the scale of the angstrom unit. Densities are calculated rather than measured because direct measurements typically yield inconsistent results. The calculated value of 5.683 is at the upper limit of the mineralogical range of 5.5–5.7 (Schueller 1954), values presumably determined by Archimedean measurements of crystals ~ 0.1 to 1 cm in size. However, at the intermediate scale of the micrometer, no invariant density is appropriate.

Ordinarily, one assumes that the surface (topological) area of a growing crystal is a function of the square of the mean radius, whereas the topological volume is determined by the cube of the mean radius. Since there is an increase in free energy with surface area, and a decrease in bulk energy with volume, there must be a critical radius giving $f_1(r^2)=f_2(r^3)$, that divides the region of thermodynamic stability with growth from the region of thermodynamic stability with dissolution, *i.e.*, the nucleation hump.

However, if there is neither surface nor volume, there can be no surface energy or volume energy. Therefore, in the circumstances needed for the formation of snowflakes, ordinary analysis finds no critical radius for growth and no requirement of a nucleating seed for growth. The discrepancy with our experience of the significant role of nucleation in meteorological phenomena says more about ordinary analysis than about nature.

The mass of the fractal snowflake model is directly proportional to the length and number of the linear segments that make it up, *i.e.*, to the total length, which (for the simple crowfoot) doubles with each recursion. Note also that after only a few recursive steps at the scale of the illustrations the overall symmetric pattern (habit) of the snowflake undergoes little or no change with further stages of recursion. Major differences in the mass of the whole unit relative to another snowflake, or major differences in the number of recursions of a single branch or even of a portion of a branch relative to the rest of the snowflake, are effectively masked. The invariant dimensionality of the pattern is given exactly by Mandelbrot's (1983) fractal dimension D_f, the logarithm of N divided by the logarithm of the scale factor: $\ln 4/\ln 2 = 2$ for the case of the simple crowfoot.

The fractal dimension is less for generators with shorter arms, as in Figure 2. It reaches the limit $D_f(1)$ for the straight line with branch length 0. Natural self-similar fractals have been considered to be random with respect to scale, that is, fractal patterns such as cloud formations are scaling in the statistical sense. The scaling for the snowflakes illustrated, as well as the angles of the patterns, are fixed by the parameters of the regular hexagonal cell. The variations in pattern between snowflakes is a result of variations in the proportionate lengths of the generator segments.

Icosahedral Shell Packings, *ISP*

Two icosahedral configurations described by Mackay (1962) lend themselves admirably to a further extension of the concept of hierarchic and scaling self-similar structure. The first arrangement, Mackay calls icosahedral shell packing, designated *ISP*. Twelve spheres (atoms) are placed at the vertices of a regular icosahedron (Fig. 4a) surrounding a single sphere or atom at the core. Eleven of the twelve, shown in Figure 4a, illustrate the symmetry (the twelfth is hidden directly below the center). Referring to the figure, each pair of opposite spheres defines one of six five-fold axes of rotation. The centers of every three tangent spheres are the corners of one of the twenty equilateral triangles that form the icosahedron's sides (fifteen of the twenty may be traced on the Figure). Twenty-five of the thirty edges are visible. The symmetry includes fifteen axes

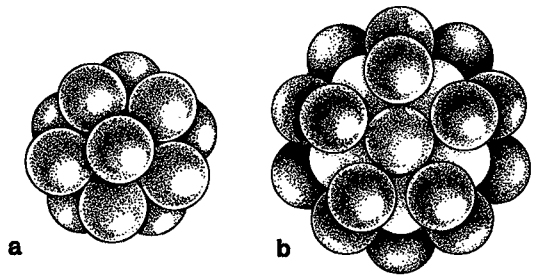

FIG. 4. (a) An icosahedron of 12 equal spheres. The radius ratio of the enclosing spheres to the largest sphere which may fit at the core is f (f is the Fibonacci ratio 1.6180...). (b) A single sphere is placed above and in contact with the three spheres of each of the 20 triangular faces of the icosahedron of Figure 4a, converting each of the 20 triangles into a regular tetrahedron. The lines joining the centers of spheres in contact form the polyhedron of Figure 6d below.

of two-fold rotation joining the centers of opposite edges. Each five-fold axis is the common line of intersection of five planes of reflection; each three-fold axis is the common line of intersection of three planes of reflection. Each plane of reflection is common to two five-fold axes and two three-fold axes.

A core sphere or a hole *coordinated* by a surrounding icosahedral shell is the starting configuration for a succession of icosahedral shells made by superposing successively larger icosahedral shells of spheres. The atoms of the twenty equilateral triangles of each shell are in a trigonal net arrangement superposed over the interstices of the trigonal net of the next smaller shell within, as in cubic close packing (*ABCA*..). Figure 5 is a view, from within, of part

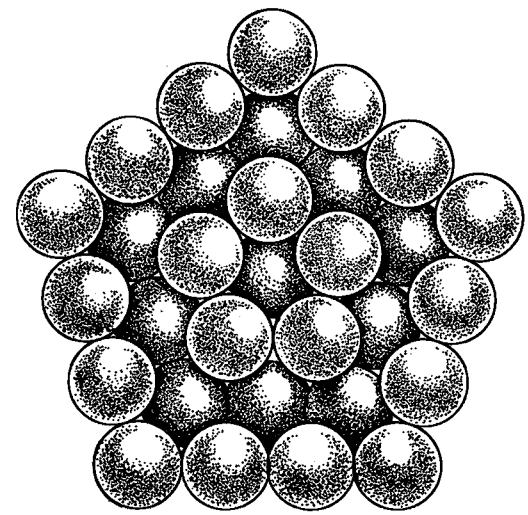

FIG. 5. Inside view of the pentagonal pyramidal cap of an ISP_3 showing six spheres of the cap of the included IS_2.

of the second and third shells of an icosahedral shell packing. The complete packing, for any number of shells, has the full symmetry of the icosahedron, namely $5m3$. The number n of spherical units in the mth shell (IS_m) is $10m^2+2$ or 12, 42, 92, 162,..., whereas the total number of units in the packing structure ISP_j is given by the sum $1 + n_m$ for $m=1$ to j. Numerical tables for *ISP* are given by Mackay (1962) and Hoare (1979). Icosahedral shell packing rather than close packing has been shown to be the stable configuration for microclusters of 13 and 55 atoms, with 12 and 42 atoms, respectively, in the outer shells (Hoare 1979). The packing of a single sphere by a shell of 12 spheres of the same size at the corners of an icosahedron (Mackay's ISP_1) is a minor distortion of the coordination of a single sphere by a shell of twelve spheres at the corners of a cubo-octahedron, the arrangement of cubic closest packing. For ISP_1, the spacing of the shell spheres is ~5% greater than their diameters, a spacing imposed upon subsequent shells. The ratio of the side of the icosahedron to the center-vertex radius is 1.051 because the central angles of the sides of the tetrahedra (with the twenty equilateral triangles bounding the regular icosahedron as bases) are ~63° instead of 60° (Mackay 1962).

The extension in intersphere spacing reduces the thickness per shell and, therefore, the packing ratio from the ideal c/a (1.63..) of closest-packing. MacKay (1962) shows the density decreasing asymptotically to a value ~8% less than that of closest packing. Although hierarchic, icosahedral shell packing does not in itself exhibit the symmetry of self-similar scaling. Mackay noted that the coordinations of vertex atoms, edge atoms and face atoms are distinct, and their proportions vary with the order of recursion, so that the physical and chemical properties of these simple but rigorously ordered structures are not constant within the boundaries of the specimen.

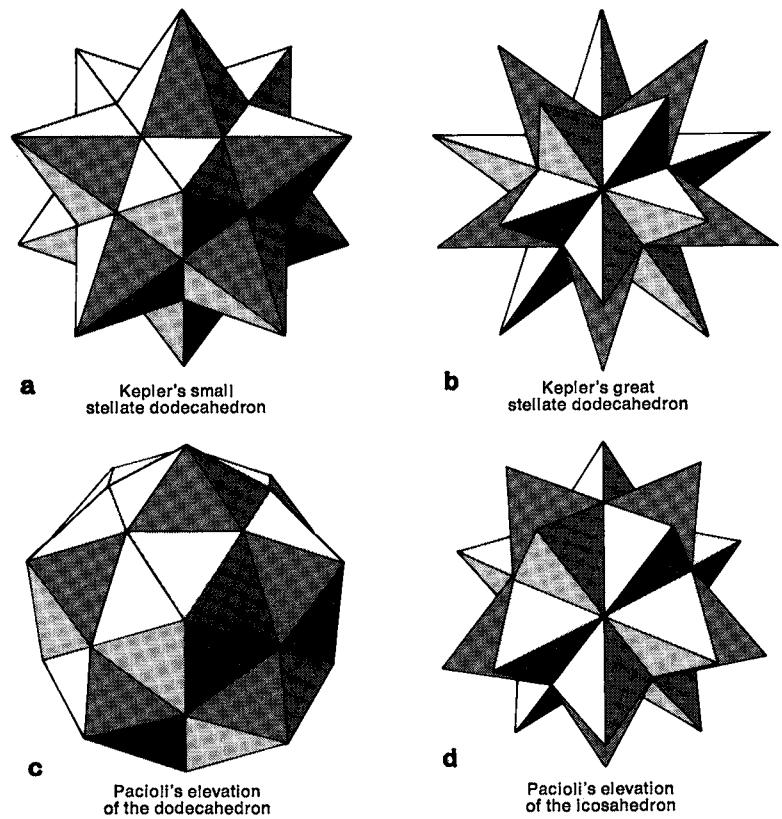

FIG. 6. The regular starred polyhedra of Johannes Kepler (a and b) and the polyhedra constructed by Leonardo da Vinci for Luca Pacioli (c and d). Pacioli raised (Lat. *elevare*) each face of the dodecahedron with a pyramid of five equilateral triangles (c) and raised the icosahedron by capping each face with a pyramid of three equilateral triangles (d). Kepler stellated the same forms by extending the faces and edges until they intersected. Reproduced from Schneer (1983).

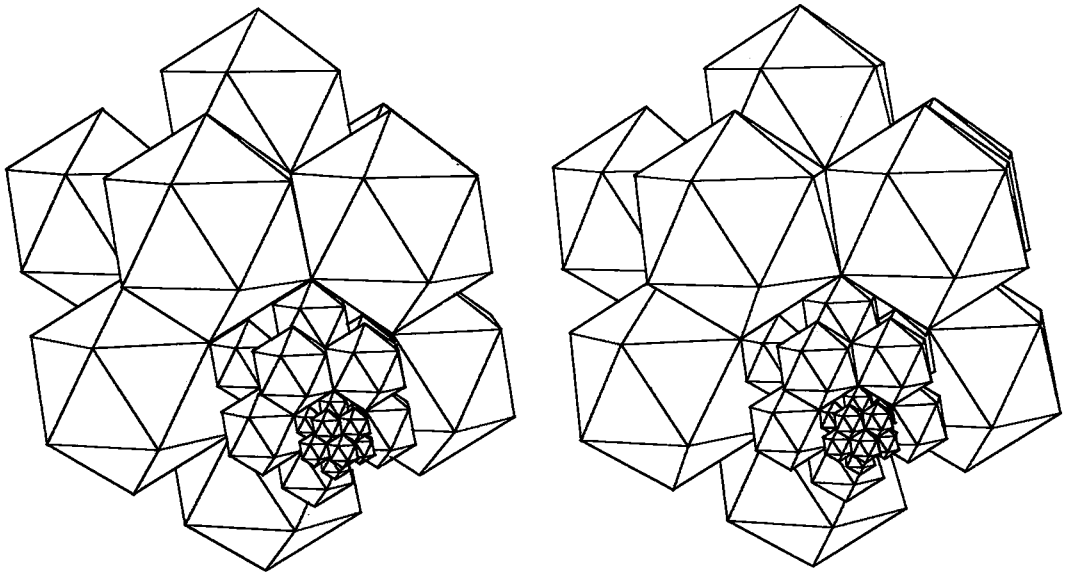

FIG. 7. A stereo pair of self-similar scaling icosahedra. Twelve icosahedra of any order p are the vertices of a single icosahedron of order $p + 1$. Each icosahedron of order p is constructed of 12 edge-sharing icosahedra of order $p - 1$. The 12 centripetal vertices of every twelve icosahedra of order p are the vertices of a regular central icosahedron of edge $1/f$ times the edge of the outer icosahedra. The edges of icosahedra of order p are f^2 times the edges of icosahedra of order $p - 1$.

If a single atom is placed over the center of each triangular face of the first icosahedron shell (IS_1), as in passing from Figure 4a to Figure 4b, the packing sequence normal to each face is the hexagonal *ABA*. Each face of the icosahedron has been converted to the base of a regular tetrahedron, the whole forming the *icosahedron elevatum* (Fig. 6d) constructed by Leonardo da Vinci for Luca Pacioli's *De Divina Proportione*. Since the regular dodecahedron is the *dual* of the icosahedron, (the vertices of the one at the centers of the faces of the other), there is another way to view the structure. The 20 superposed atoms are the vertices of 12 pentagonal faces comprising a second, dodecahedral shell, with each face dimpled inward to a vertex of the original icosahedron (IS_1). Each vertex of IS_1 is the apex of a concave pentagonal pyramid of equilateral triangles, *i.e.*, an indent or dimple. There are 20 + 12 or 32 external atoms surrounding the core. Placing 12 more atoms in the 12 dimples makes a third shell, the icosahedral dual this time, with vertices directly above (*i.e.*, out from) the vertices IS_1. The surface configuration is now that of Leonardo's *dodecahedron elevatum* (Fig. 6c), again with 32 atoms. Each of the 12 faces of the second-shell dodecahedron is capped by a convex pentagonal pyramid of equilateral triangles. Alternatively, the 32 atoms of either the convex or the concave dodecahedron may be visualized as the vertices of a mutually interpenetrant dodecahedron and icosahedron with coincident symmetry-elements. The surface structure is a tiling of a spherical surface by 12 regular pentagons, as in a regulation volleyball, and a tiling of 20 equilateral triangles with corners central to the pentagons. The atom at the core of all the shells is icosahedrally coordinated by IS_1, but it is also the common vertex of 12 icosahedra coordinating each of the 12 atoms of IS_1. These atoms are in mutual icosahedral coordination, readily seen in simple ball-models.

Other varieties of pentagonal packings of spheres include: (1) the successive pyramidal shells revealed by slicing *ISP* through a pentagonal cross-section (as in Fig. 5), and (2) the shells generated by adding layers to the pentagonal bipyramid formed from one sphere above and one below a pentagon of five (which is the stable configuration for a seven-atom microcluster; Hoare 1979).

A FRACTAL ICOSAHEDRAL STRUCTURE

The second of the two hierarchic configurations described by Mackay (1962) is an icosahedron constructed of 13 icosahedra, each made of 12 icosahedra enclosing another icosahedron, *etc.*, always with common symmetry (Fig. 7). Because Mackay attributed the idea to J.D. Bernal, the configuration is identified below as the Bernal icosahedron *B*. As the icosahedron is a quasispherical form, it should be possible to arrange 12 icosahedra of any order of recursion p at the corners of a larger icosahedron

of order $p+1$. With the 13 icosahedra of any order sharing edges and vertices (Hiraga *et al.* 1985), each icosahedron of side length s_p is a shell of 12 icosahedra of side length:

$$s = 2s_p[1+\sin(\pi/10)] \text{ (Hiraga } et\ al. \text{ 1985)}$$
$$= s_p/\mathbf{f}^2; \mathbf{f} \text{ is the fibonacci ratio } 1.618033989\ldots, \quad (1)$$

the limit of the Fibonacci sequence, also called the Golden Mean.

The hierarchic self-similarity is shown in Figure 7. Each icosahedral dozen of stage p encloses a core icosahedron with the configuration of stage $p-1$. The radii of the concentric icosahedra (*i.e.*, of the spheres circumscribing the icosahedral shells of each successive stage) are in the ratio

$$r_p/r_{p-1} = \mathbf{f}^3 \quad (2)$$

If equations (1) and (2) hold for p of any integer, the structure is a fractal. The numbers of atoms for $p>0$ in the trivial case without edge or corner sharing increases exponentially with p. Assuming a lowest cutoff at $p(1)$ with an atom of Mn icosahedrally coordinated by 12 Al as the first icosahedron, the proportion $AlMn_{0.085}$ is constant with growth. There are 12^p atoms of Al and 13^{p-1} Mn for each order of recursion p. Proportions for edge and corner sharing are calculated below (Table 1).

If the *SSC* icosahedron without vertex sharing is considered as an ordered fractal dust of points of topological dimension 0, then from Mandelbrot's definition (1983), the fractal dimension is $\ln 13/\ln \mathbf{f}^3 = 1.7767\ldots$

Using the notation B_p for the *SSC* icosahedron of order p, B_2 would represent the structure that, with edge and corner sharing, has been proposed by Hiraga *et al.* (1985) as a possible structure for melt-quenched AlMn alloys exhibiting pentagonal symmetry (shechtmanite). Electron micrographs and diffraction patterns exhibit icosahedral symmetry and the Fibonacci proportions. In the model of the proposed structure presented by M. Hirabayashi at the Oji International Conference in 1985, there is a core icosahedral shell of 12 aluminum atoms corresponding to the $B1$ configuration without a central core. Twelve $B1$ icosahedra with core atoms of Mn surround the central B_1, keeping the same orientation of symmetry for all icosahedra, to form the next order of icosahedron, B_2, by edge- and vertex-sharing. If the icosahedron of the stereo pair of our Figure 7 is order $p = 5$, then the 12 next largest icosahedra are fourth-order, one of which is subdivided to show its construction of 12 third-order icosahedra, one of which is subdivided to show 12 second-order icosahedra, the inner vertices of each of which constitute initial first-order icosahedra. As above, the numbers of Mn core atoms are given by 13^{p-1} (less one for the Mn omitted from the central $B1$). The numbers of Al atoms are less than 12^p because of the edge- and corner-sharing. For every 12 icosahedra of order p surrounding a core icosahedron of order $p-1$, there are 12 vertices common to the 12 vertices of the core icosahedron; 5×12, or 60, of the 12×30 edges are shared by two icosahedra, and the 60 vertex corners of the shared edges are shared by 3 icosahedra. There are 2^{p-1} edge atoms per shared edge for orders $p>2$. The stoichiometric values are

$$Al_p = 13Al_{p-1} + 8 - 30(2^{p-1}), \textit{ cf.} \text{ Table 1.}$$

The stoichiometry $AlMn_{0.143}$.. reported by Hiraga *et al.* (1985) for "...144 fundamental icosahedrons of $Al_{12}Mn$.." is reached if the structure of B_2 is incomplete. The growth of B_2 may be visualized as proceeding by the addition of five concentric spherical shells of atoms (counting the core atom or vacancy as zero and the 12 coordinating atoms about the core as the first). It is the Leonardo–Pacioli development of IS_1 described above. The addition of Al above the center of each of the 20 triangles of B_1 makes a second atomic shell with pentagonal pyramidal dimples, *i.e.*, the icosahedron elevatum. The addition of a third shell of 12 Mn in the pyramidal dimples changes the configuration to the dodecahedron elevatum with Mn for the apices of the pentagonal pyramids, and the Al pentagons of the second shell as their bases. The Mn/Al atomic ratio is 0.375. Another shell of 12 pentagonal rings of Al is placed with pentagon centers above the Mn, making a fourth shell with 60 Al (these rings do not share elements). Each pentagon of the fourth shell is rotated 36° about its center with respect to the Al-pentagon of the second shell, below. The addition of a single Al centered above each of the 12 pentagons completes B_2. The Mn/Al ratio shifts with each atomic shell and reaches 0.115.. for 5 complete shells.

The structure should be extremely strong. Each of the Mn is icosahedrally coordinated by the 12 Al of IS_1. Each of these 12 Al is itself at the center of a distorted icosahedron. The 12-coordination is by the core atom (or vacancy if no atom is present) and the pentagonal ring of its neighboring Al of IS_1 below, and a pentagonal ring of Al of the second atomic shell capped with a Mn of the third shell, above. The size of the outer capped ring is f times that of the inner capped ring, hence the distortion which, however, does not alter the icosahedral symmetry of the whole.

The total numbers of aluminum atoms in the sur-

TABLE 1. ATOMIC PROPORTIONS FOR *SSC* ICOSAHEDRAL SERIES

	p	Mn	Al	at. ratio	Mn+Al
B_1	1	1	12	.085	13
B_2	2	13	104	.125	117
B_3	3	169	1240	.136	1409
B_4	4	2197	15888	.13828	18085
B_5	5	28561	206072	.13860	234633

face atomic shells of the *SSC* icosahedra are not the same as those cited by Mackay (1962) for icosahedral shell packing, *cf.* above. We find the *SSC* numbers: 12, 72, 312, 1032,... for $p = 1, 2, 3, 4,..$ (Fig. 7). Therefore the two structures may be distinguished by their surface properties.

Structures Combining *ISP* and *SSC*

We find an infinite number of potential self-similar scaling icosahedral structures starting with lower cutoff icosahedra made of Mackay's icosahedral shell packings of any order m; $m = 1,2,3,...$ Using B without subscript to represent the Bernal recursion, these structures are as follows:

$B(ISP_1)$ = *SSC* icosahedral series, the points of which are icosahedra of 13 points (ISP_1).

$B(ISP_2)$ = *SSC* icosahedral series, the points of which are ISP_2.

$B(ISP_3)$ ....

These compound structures have the *SSC* symmetry of the Bernal recursion. We may also conceive of an infinite series of *ISP* structures, the packing units of which are *SSC* icosahedra of order 1,2,3,... *etc.* If the lower cutoff icosahedron with 1 center and 12 corners is order $p(1)$, then the single center is order $p(0)$. Using *ISP* unsubscripted to represent the Mackay hierarchy, these structures are designated:

$ISP(B_0) = ISP_1$; points of the icosahedral shells are single points. There is one center.

$ISP(B_1)$: points of the icosahedral shells are the $ISP(B_0)$ or B_1 above. To the extent that a self-similar scaling recursive structure B_p may be considered a fractal even for small values of p, it is a packing of fractals, even if the packing itself is dimensionally classical.

$ISP(B_2)$ ....

The icosahedral shell packing of icosahedral shell packings of any order is also possible.

$ISP(ISP_m)$, $m = 0,1,2,....$

As in the phenomenon of polytypism with periodic alternation between sequences of two elements c and h, the B series and the *ISP* series are conceivably subject to alternation in a single structure. Further complexity could be introduced because the quasispherical icosahedral microclusters of any order may be the structural elements for cubic and hexagonal close packing and their polytypic alternations.

Icosahedral Symmetry of Viral Infections

According to summary texts (*cf.* Becker 1982), the external shells called *capsids* of the majority of virus particles (virions) exhibit icosahedral form and symmetry. The equilateral triangular sides of the icosahedral capsids are made of structural units called *capsomeres* in the trigonal net arrangement of *ISP*. The numbers of capsomeres of the capsids are diagnostic for the virus species. They fall in the same series as IS_m with n or the number of capsomeres = 12, 42, 92,... for $m(1,2,3...)$. The structures of the capsomeres themselves are poorly understood, but in electron micrographs, they may appear as uniform quasispherical particles with a hexagonal(?) outline conforming to the symmetry of the icosahedron projection on a face. At the next hierarchic level of the virus structure, the icosahedral virions may be aggregated as crystals within the host organism, most commonly observed as one or several layers of virions in a) trigonal- or b) square-net arrays. The structure has been interpreted as ordinary close-packing in a) cubic [111] or hexagonal [0001], or b) [001] sections. However, no one has yet considered that the icosahedral symmetry of the individual virions, that is of the next lower hierarchic order of structure, imposes the higher $5m3$ symmetry of the compound icosahedral structures discussed above, just as the full $m3m$ symmetry is expressed in a cubic close-packed array, however fragmental its expression.

One unusual electron micrograph (Melnick *et al.* 1968) shows five(?) concentric pentagonal rings of icosahedral virions of *Herpes simplex* (Fig. 8). There are 8 or 10 particles along the edge of the outer pentagon edge, and two along the innermost. (Because the infection merges into the host, the precise boundary is not that obvious to a mineralogist.) The micrograph was originally described as showing a section normal to the pentagonal axis of a pentagonal dipyramidal packing. However, this arrangement of the virions is the same as that for a section in the plane of the pentagonal ring of an icosahedral shell packing macro-unit (or a fragment of a macro-unit). Pentagonal rows for alternate shells are in the plane of the section, with the intervening shells above or below. Taking an outer row of 10 virions to the pentagon edge for the boundary, the row would be an edge of an IS_9 with 812 virions, about 8 successive concentric shells the innermost of which would be IS_1 with 12 virions. Although the two arrangements for the virions of the micrograph are the same, the 3-fold axes of the icosahedron preclude the reflection perpendicular to the 5-fold axis of the dipyramid. Since each *Herpes* virion is itself known to be an icosahedron with a 162-capsomere shell, IS_4 (Becker 1982), the structure proposed here is $ISP_9(IS_4)$. Other micrographs showing the trigonal and square nets of packing arrays could be interpreted as sections, or fragments of sections, through packing arrays on one of the 20 faces of an *ISP* macro-unit. The distinction does not depend upon the overall morphology of the specimen, which is in any case incomplete, but on the symmetry. The symmetry is icosahedral ($5m3$) if the degenerate symmetry is icosahedral, that is, if the virions are icosahedral and their orientation is compatible (as in *ISP*).

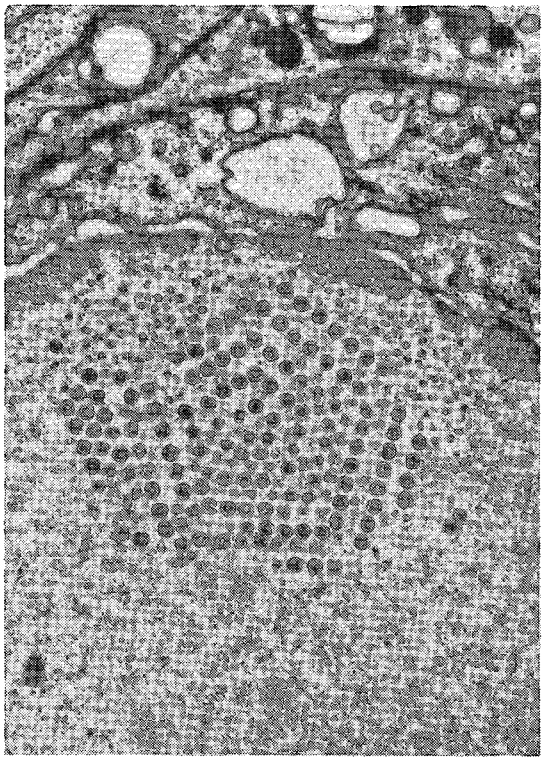

FIG. 8. Hierarchic structure in the cancerous liver of a mouse. The electron micrograph, reproduced with kind permission from Melnick *et al.* (1968), is of an aggregate of virions of *Herpes simplex*. Each virion is an icosahedron with an outer shell of 162 capsids (IS_4). Comparing with Figure 5, the infection is apparently an $ISP_9(IS_4)$ structure.

Similarly, crystallographers have commonly classified inorganic pentagonal structures as fiveling twins. The distinction lies in whether or not the 5-fold symmetry is an intensive property, *i.e.*, whether it crosses the twin boundaries or is limited to the single axis at the center of the specimen. The virus infection of Figure 8 is properly considered icosahedral shell packing rather than pentagonal pyramidal packing because the units of structure, in this case the virions, are icosahedral. The degenerate symmetry of the pentagonal dipyramid ($5/mm$) is incompatible with the icosahedral symmetry of the virions.

Extending this reasoning to other species of virions with hierarchic surface-structure, the 252-capsomere surface (IS_5) is the pattern of the *Adenovirus* capsid. The *Tipula iridescens* capsid is an icosahedron with 812 capsomeres (IS_9). The 72 capsomeres of the icosahedral surface of the *Papovavirion* corresponds to the number of spheres in the outermost surface of a second-order *SSC* icosahedral structure, B_2. There are 32 capsomeres to the *Parvovirion* with the same symmetry as the icosahedron (Becker 1982). This symmetrical arrangement of 32 spheroids is only possible with the two interpenetrant dodecahedron-icosahedron arrangements described above (or the two Keplerian regular solids of Fig. 6, which are steeper versions of the Leonardo solids). If the icosahedral vertices are the apices of convex pentagonal pyramids, the form is Leonardo's *dodecahedron elevatum*, but if the pyramids are concave, it is the *icosahedron elevatum* with a proportionately smaller mass.

SELF-SIMILAR SCALING IN HEXAGONAL AgI (IODARGYRITE) FLAKES

Symmetrically and dimensionally almost congruent with ordinary ice, iodargyrite has the wurtzite structure: hexagonally close-packed iodine with interstitial silver in mutual tetrahedral coordination. The space group is $C6_3mc$. The point group is $6mm$. The projection of the structure on the basal plane (0001) is a hexagonal tiling, with nodes alternately Ag and I. The tiling is dense, *i.e.*, the hexagons cover the plane without holes. The cell dimension a equals 4.5922 Å (Swanson *et al.* 1959) with the effective radius of the iodine 2.2961 Å. The side of the unit hexagon is 2.6513 Å, and its diameter, 5.3026 Å. The interplanar spacings are so close to those of ice that the X-ray powder-diffraction lines for the two species are almost coincident, verified when some of our low-temperature X-ray studies of the AgI crystallites showed contamination by frost. Originally, we had prepared dendritic snowflake-like crystals of iodargyrite in a saturated aqueous KI solution by letting it warm from 0°C to room temperature, a procedure found to yield material with 99.6% hexagonal ($2H$) X-ray diffraction pattern (AgI is ordinarily polytypic, Schneer & Whiting 1963). On recent examination with SEM, two habits were observed, the 'rusty nail' (Fig. 9) and the 'snowflake' (Fig. 10), both resembling habits of snow crystals.

Figure 1 is our electron micrograph (SEM) at 5000× of the dentellated flake shown in Figure 10b at a magnification of 60×. The enlargement is focused southeast of the center of the flake, about halfway to the edge. At 5000×, the frond-like flake of Figure 10b becomes a sheeting of nets successively superposed to yield negative hexagonal prisms (holes). The hexagonal network tiling of Figure 11 was inspired by a cubic fractal distribution of points discussed by Mandelbrot (1983, pp. 95, 96) as an idealized model for the distribution of matter in space (Fournier dust). In Figure 12 the hexagonal cells of the *SSC* net outlines of Figure 11 were drawn with $3.5 \times 10^{-4} \times 5000$ cm diameters and superposed over Figure 1. The structural hexagonal cell of AgI, repeated recursively as in the self-similar scaling hexagonal tiling of Figure 11, and multiplied by

3 with each ascending order of recursion, reaches the size of the superposed outline nets with the eighth order of recursion. The scale factor of 3 is set by the geometry of the hexagon.

$$\text{dia.}_p = 5.3026 \times 10^{-8}\ \text{cm} \times 3^8 = 3.4790 \times 10^{-4}\ \text{cm}$$

The point symmetry of the structure is expressed by the union of the crystallographic point-group symmetry with the dilational *SSC* symmetry operation: [*6mm*:*SSC*].

The wurtzite structure is polar in the direction perpendicular to the plane of tiling. Interpreting the doubled flakes of Figures 10a and 10b as composite crystals, probably twins, I have designated the surface of adhesion of the dendrite as negative because of the concavity of the details at high magnification. The negative surface revealed in Figure 1 is constructed of superposed hexagonal nets with enough long-range order to impose the macrosymmetry of the flakes. Note that the long- and short-range order of X-ray and electron diffraction is unaffected by the *SSC* symmetry.

The dentellated flake of Figure 10a is (apparently) in the opposite or positive orientation, with its back to the viewer. Figures 13a and b are electron micrographs (TEM) of a positive surface (not the same flake) at 2000× and 20000×; they reveal self-similar scaling of the convexities which are the reverse side of the concavities of Figure 11. To verify this polar interpretation, another composite flake was prepared

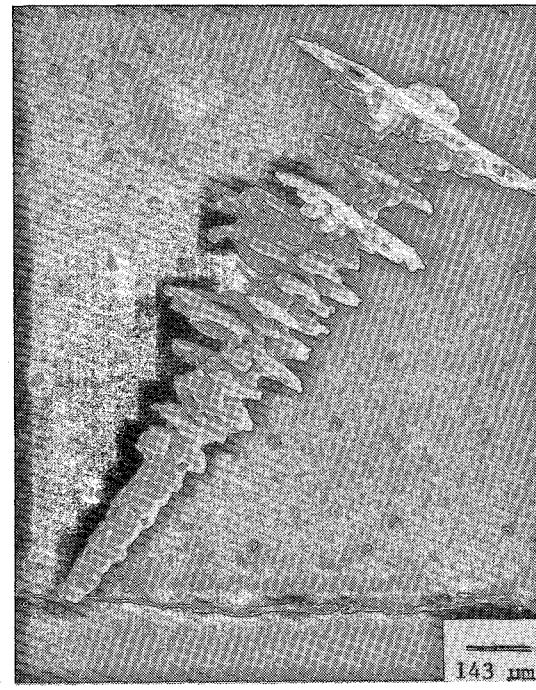

FIG. 9. AgI flake with rusty nail habit. One of the two habits of AgI precipitated with the warming to room temperature of solutions of AgI in KI and water saturated at 0°C. Polaroid original at 70×.

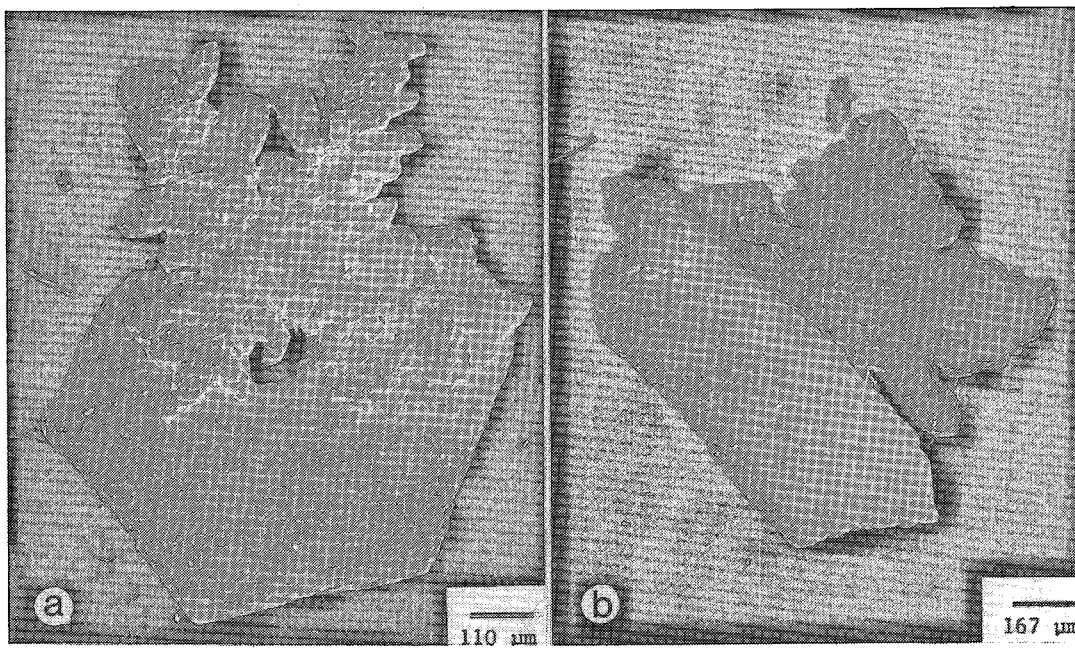

FIG. 10. Composite AgI 'snowflakes'. A hexagon flake is joined with a dendrite. The composite pairing and the central hollow in the hexagon flake of (10a) are typical. In (a) the dendrite covers the hexagon; the positive side(?) (convexities) of the dendrite faces up. In (b) the hexagon overlies the dendrite. The negative(?) side (concavities) of the dendrite faces up.

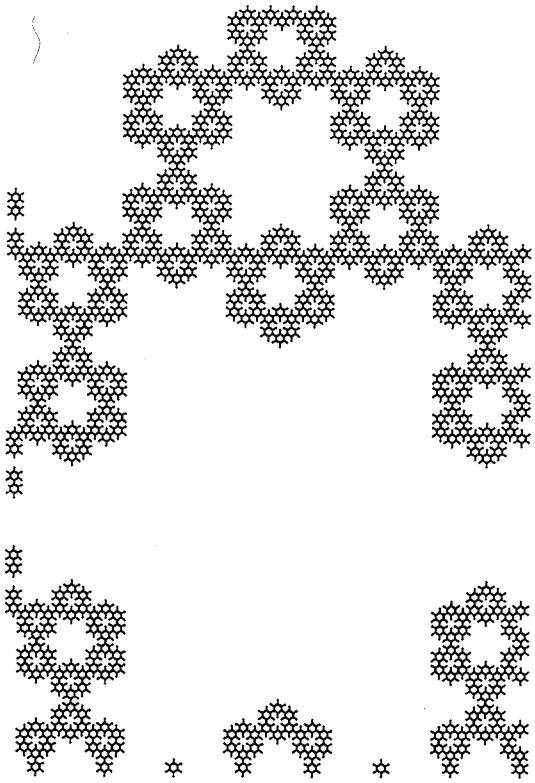

FIG. 11. A self-similar scaling (*SSC*) hexagonal net. The nodes of each hexagon of order p and side length s are hexagons of order $p - 1$ and side length $s/3$. Each hexagon of order p is the node of a hexagon of order $p + 1$ and side length $3s$. The Hessel point-group symmetry is $6mm$ which commutes with the dilational symmetry operation, *SSC*. The hypersymmetry is $6mm$:*SSC*.

to view the negative side (Fig. 14, SEM 5000×). The concavities of the specimen suggest crystallization by a condensation or 'curdling' process (approximating the self-similar scaling process that Mandelbrot (1983) used to construct a fractal 'gasket'). A polygonal initiator is divided into a central polygon with similar bounding polygons. The material of the central polygon is removed (leaving a 'trema') and is divided among the bounding polygons. The process then repeats for each of the bounding polygons. Applying Mandelbrot's process to an initiating hexagon of six triangles leads to Figure 15. Starting with a uniform (Monte Carlo) distribution of matter throughout the 2-dimensional space of each triangle, divide each side by 3 and join adjacent points of subdivision to form an interior hexagon and three equilateral triangles. The material of the hexagon is distributed uniformly among the three triangles. Continue the process for each of the triangles by taking the matter of the central hexagon and assigning it to the three bounding triangles. This is the recursive process involving condensation and ordering which was designated *analytic* above. The same pattern is achieved *synthetically* by the radial addition of cells according to a preset rule, a process defined as 'cellular automaton evolution' (Wolfram 1984).

SELF-SIMILAR SCALING OF PENTAGONAL AlMn ALLOYS

At least some of the class of melt-quenched AlMn alloys with pentagonal symmetry (shechtmanite) display structure, at the micrometer scale, remarkably similar to the self-similar scaling hexagonal frameworks of AgI and snow. Although the icosahedral model proposed by Hiraga *et al.* (1985) might suggest an oolitic or reniform habit for their $AlMn_{0.143}$ alloy, their observations at lower magnification revealed a frond-like conformation not unlike that of the AgI flake of Figure 10a. Figure 16 is an optical micrograph of Al_7Mn alloy at 4000× showing "shechtmanite 'snowflakes'..." (Nelson 1986). The anomaly is resolved if the structure is considered as a dilational tiling at the micrometer scale, *i.e.*, a pentagonal version of the tiling in Figure 11. The 2- and 3-dimensional Penrose tilings might still be the basis for the atomic structure of shechtmanite (Levine & Steinhardt 1984, Ogawa 1985), yet this would not

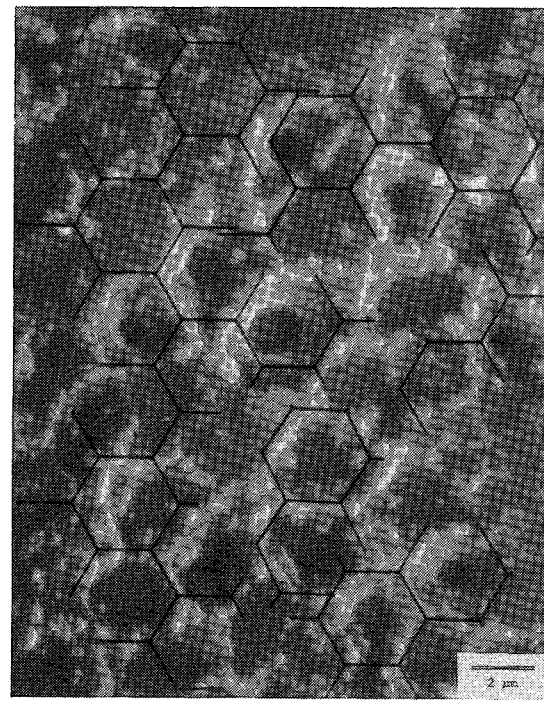

FIG. 12. The AgI nets of Figure 1 referred to *SSC* hexagonal tiling. *SSC* hexagonal nets of the 8th order starting with the unit hexagonal AgI cell as first order, are superposed on the electron micrograph of Figure 1.

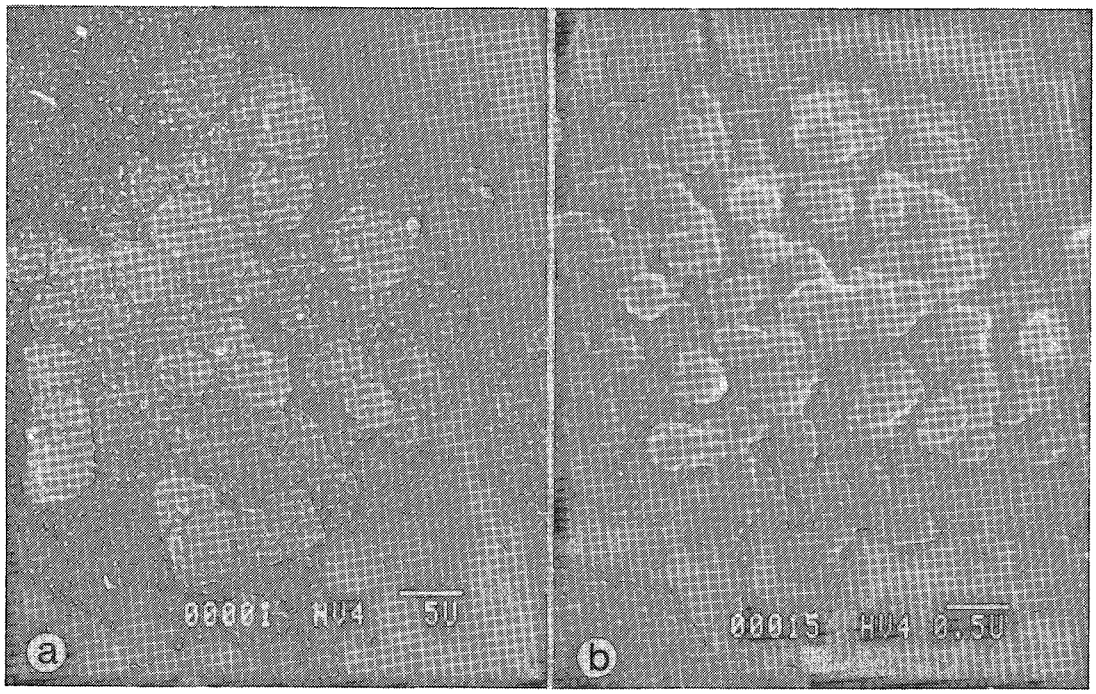

FIG. 13. The positive side of an AgI flake. The concavities of Figure 1 are the self-similar scaling convexities of Figures 13a and 13b.

preclude an extensive point group for the configuration shown in Figure 16. Figures 17 and 18 are examples of pentagonal tilings with the requisite dilational symmetry.

As in the cases of the hexagonal structure discussed above, the pentagonal *SSC* symmetry does not abrogate short- and long-range order so that clear diffraction records are possible. Figure 17 illustrates a dilational, hierarchic, pentagonal tiling of B_1 icosahedra linked by edge-sharing (with concomitant variance in the shell-to-core atomic ratio). The pattern of Figure 17 is equivalent to a thin section, one B_1 icosahedron thick, taken through a B_5 icosahedron at the level of the upper rim of the upper pentagonal ring of five B_4 icosahedra. Doubling the width to include the next slice above would show an additional B_1 to fill each of the smallest of the pentagon holes. The two-dimensional symmetry of the slice is *SSC*:5*m*, whereas the three-dimensional icosahedral symmetry of *SSC*:5*m*3 extends as far as the thickness of the slice.

A hierarchy of *SSC*:5*m* tilings is possible, as for example that of Figure 18, with pentagons of order p with sides of three rather than two pentagons of order $p-1$, or four, *etc.* Such an increase emphasizes the large polygonal holes (negative crystals) observed under given conditions, masking if not eliminating the smaller holes of the girdling space. Stringing out the lengths of the sides of hexagons

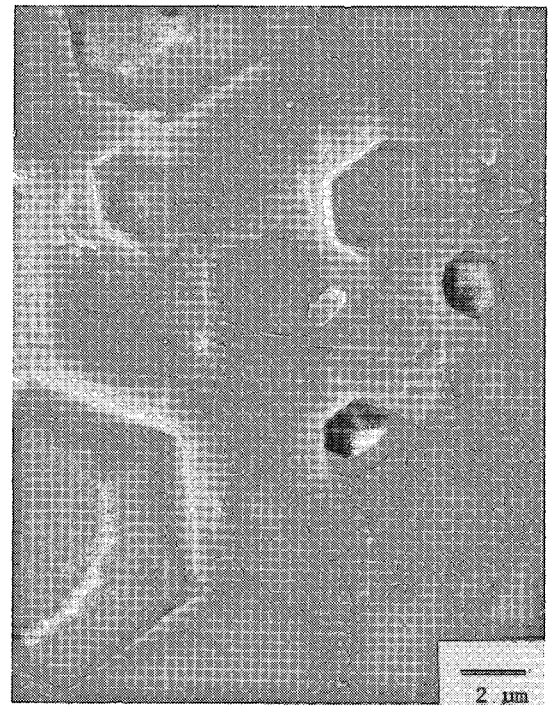

FIG. 14. The negative side of an AgI flake.

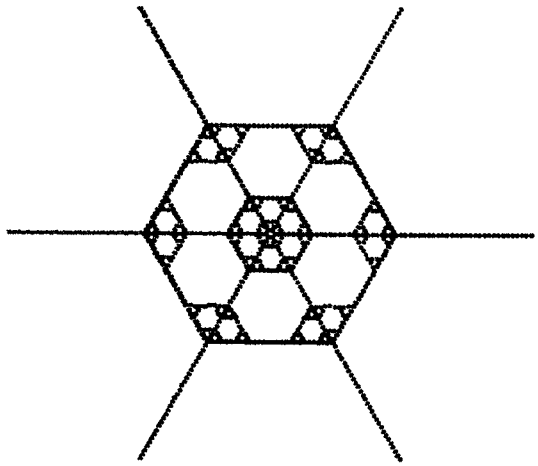

FIG. 15. An ordered fractal produced by condensation/ordering. The material of the largest hexagonal space to fit each of the six triangles of the hexagonal initiator is divided among the interstitial triangles. The process is repeated within each triangle and each of the resulting triangles *etc.* The process is called 'curdling' by Mandelbrot. The figure is illustrative of a class of curves also produced (as in the algorithm to plot this figure) by adding uniform cells outward from a central core according to preset rules of succession as in cellular automaton evolution (Wolfram 1984).

of intermediate order would account for the distribution of negative hexagonal prisms observed at the micrometer scale in iodargyrite, as in Figure 14.

The fundamental icosahedra of the tilings of Figures 17 and 18 could be themselves *B* or *ISP* icosahedra of higher order than one. The linkage of icosahedra with edge sharing is also possible in planes perpendicular to any of the ten three-fold axes of the icosahedron. Other linkages are possible and even probable, as for example, chains parallel to a five-fold axis by corner sharing, or the sharing of corner or edge icosahedra of order p by icosahedra of order $p + 1$, *etc.* The vertex/core atomic ratio (stoichiometry) would vary with the linkage. The two-dimensional tilings may also be considered as pentagonal rings enclosing pentagonal holes of the same orientation. The ratio of the thickness of the rings to their diameters is a function of the compounding of the hierarchic structure of the tiling, as in stringing out the lengths of the sides of the pentagons of the highest order. The pentagonal rings are also the sides of pentagonal dodecahedra, the three-fold vertices of which are clearly visible in Figure 16.

CONCLUSION

The ordinary snowflake, iodargyrite flakes, a number of virions, "shechtmanite" flakes and "quasicrystals" of melt-quenched $AlMn_{0.143}$.. exhibit evidence of hierarchic structures ranging from simple icosahedral shell packings to the multirecursive self-similar scalings of Mandelbrot's fractals. The combination of self-similar scaling with point symmetry results in a new class of dilational symmetry groups with long- and short-range order. Examples include the *6mm:SSC* of dendritic snow crystals and iodargyrite flakes, or the *SSC*:5*m*3 of the Al-Mn alloys. Except for the dendritic snow crystal, observation of the symmetry of self-similar scaling seems to require exploration of structures at a scale greater than permitted by ordinary optical microscopy and less than the scale of X-ray diffraction. At the scale of the micrometer, the organization and properties of mineral materials may depart sharply from predictions made by extrapolation from the organization both at the scale of the molecule or unit cell, as revealed by X-ray diffraction, and at the macroscopic scale of direct visual inspection, both of which stand as limits or cut-offs to the recursion. But if these large-scale structures are rigorously ordered, how is it that they evade detection by diffraction? First, the spacings of interest are in the micrometer range, rather than that of the X-ray wavelength. Second, these structures are absent in the ideal specimens of research grade used for single-

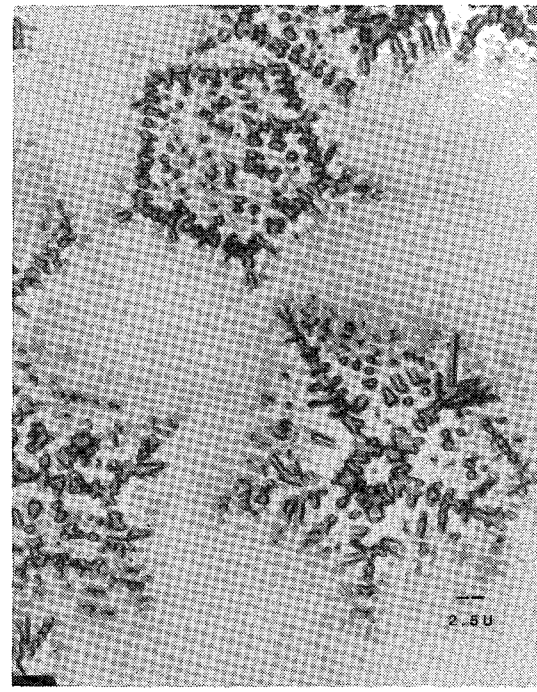

FIG. 16. Al_7Mn 'snowflake' exhibiting *SSC*:5*m*3 symmetry. Photo with permission from laboratory of Leonid A. Bendersky and Robert J. Schaefer at the National Bureau of Standards.

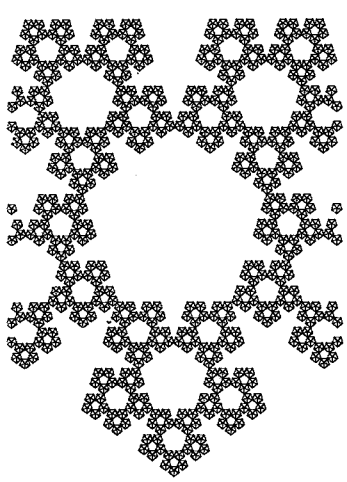

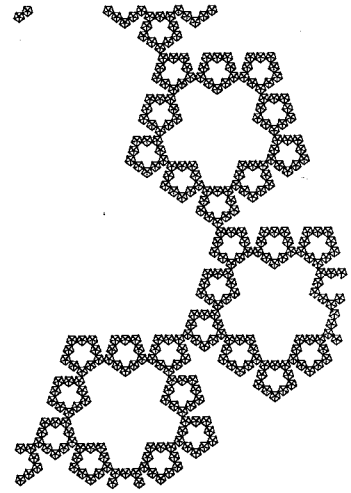

FIG. 17(left). A self-similar scaling tiling of B_1 icosahedra (with edge-sharing) showing short- and long-range pentagonal symmetry. It is the equivalent of a slice through a B_5 icosahedron, of thickness equal to a B_1. The B_1 icosahedra of the next slice above are centered on the smallest pentagon rings. Successive slices above are centered on the smallest pentagon rings. Successive slices above and below, projected on the same plane would fill all larger rings retaining the *SSC*:5*m* symmetry. The full icosahedral symmetry *SSC*:5*m*3 of the B_1 icosahedra is extended with the total thickness of the section.

FIG. 18(right). A second hierarchic level of the tiling of Figure 17. Each pentagon of order p is constructed of 3 pentagons of order $p - 1$, doubling the diameter of the pentagons at every order with respect to the pentagons of the same order of Figure 17.

crystal analysis. Third, it is possible that diffraction does indeed record the lesser spacings of dilational structures as the superlattice lines commonly observed (and ignored) in routine analyses of industrial-grade material. Finally, it was through diffraction that the recursive pentagonal symmetry of shechtmanite was first noticed.

Recursive dilation makes 'crystallographic' symmetries such as 5-fold rotation possible, and transforms invariant properties such as density, which are topologically dependent, into variables. The estimation of extensive properties such as length, area and mass requires reconsideration. In these structures, space as well as matter is configured during the process of growth, a fact of life for which field theory should have prepared us.

ACKNOWLEDGEMENTS

I am grateful to Ichiro Sunagawa and the organizers of the Oji International Conference on Crystal Morphology and Growth (Zao, Japan, 1985) for their kindness in providing a forum for the initial exploration of these ideas. Figures 4 and 5 are common geometric illustrations included here for the explanation of Figures 6 and 8. Figure 8, called to my attention by Frank Rodgers, is reproduced with the kind permission of Joseph L. Melnick. Nancy Cherim assisted with the electron microscopy. I thank Leonid A. Bendersky and Robert J. Schaefer for permission to reproduce Figure 16. The other illustrations, including the micrographs, and the interpretations placed upon them are my responsibility.

I thank the editors and referees for their detailed analyses and criticism. J.D.H. Donnay, J.V. Smith and C.S. Smith have been particularly encouraging. Facilities for these studies were provided through the College of Engineering and Physical Sciences of the University of New Hampshire. The kindness and generosity of the above institutions and individuals in facilitating the preparation of this paper is not to be construed as any indication of their approval of its contents.

REFERENCES

BECKER, Y. (1982): *Molecular Virology*. Nijhoff, The Hague.

BENTLEY, W.A. & HUMPHREYS, W.J. (1931): *Snow Crystals*. McGraw-Hill, New York.

HIRAGA, K., HIRABAYASHI, M., INOUE, A. & MASUMOTO, T. (1985): Icosahedral quasicrystals of a melt-quenched Al-Mn alloy observed by high-resolution electron microscopy. *Sci. Rep. Res. Institutes Tohoku Univ.* **A32**, 309-314.

HOARE, M.R. (1979): Structure and dynamics of simple microclusters. *Adv. Chem. Phys.* **40**, 49-135.

KOMODA, T. (1968): Study on the structure of evaporated gold particles by means of a high resolution electron microscope. *J. Appl. Phys.* **7**, 27-30.

LEVINE, D. & STEINHARDT, P.J. (1984): Quasicrystals: a new class of ordered structures. *Phys. Rev. Lett.* **53**, 2477-2480.

MACKAY, A.L. (1962): A dense non-crystallographic packing of equal spheres. *Acta Cryst.* **15**, 916-918.

_____, FINNEY, J.L. & GOTOH, K. (1977): The closest packing of equal spheres on a spherical surface. *Acta Cryst.* **A33**, 98-100.

MANDELBROT, B.B. (1983): *The Fractal Geometry of Nature.* W.H. Freeman, New York.

MELNICK, J.L., RABIN, E.R. & JENSON, A.B. (1968): Intracellular herpes-virus aggregate in the form of a pentagonal dipyramidal crystal-like structure. *J. Virology.* **2**, 78-80.

NELSON, D.R. (1986): Quasicrystals. *Scientific American* **254**, 42-51.

_____ & HALPERIN, B.I. (1985): Pentagonal and icosahedral order in rapidly cooled metals. *Science* **229**, 233-238.

OGAWA, T. (1985): On the structure of a quasicrystal – three-dimensional Penrose transformation. *Oji Int. Conf. on Crystal Growth and Morphology, Zao, Japan, Program Abstr.* 13-14.

PALACHE, C. (1932): Multiple twins of diamond and sphalerite. *Amer. Mineral.* **17**, 360-361.

SCHNEER, C.J. (1983): The renaissance background to crystallography. *Amer. Scientist* **71**, 254-263.

_____ (1985): A heuristic model of snowflake morphology and growth. *Oji Int. Conf. on Crystal Growth and Morphology, Zao, Japan, Program Abstr.* 24-25.

_____ (1988): A heuristic model of snowflake morphology and growth. *Morphology and Growth Unit of Crystals, Proc. Oji Int. Seminar on Morphology and Growth Unit of Crystals.* (I. Sunagawa, ed.). Terra Sci. Pub. Co., Tokyo (in press).

_____ & WHITING, R.W., JR. (1963): Phase transformation and thermal hysteresis in the system AgI. *Amer. Mineral.* **48**, 737-758.

SCHUELLER, A. (1954): *Die Eigenschaften der Minerale II.* Akademie-Verlag, Berlin.

SHECHTMAN, D., BLECH, I., GRATIAS, D. & CAHN, J.W. (1984): Metallic phase with long-range orientational order and no translational symmetry. *Phys. Rev. Lett.* **53**, 1951-1953.

SWANSON, H.E., GILFRICH, N.T., COOK, M.I., STINCHFIELD, R. & PARKS, P.C. (1959): Standard X-ray powder diffraction patterns. *Nat. Bureau Standards Circ.* **539**, 8,52.

WEYL, H. (1952): *Symmetry.* Princeton Univ. Press, Princeton, N.J.

WOLFRAM, S. (1984): Cellular automata as models of complexity. *Nature* **311**, 419-424.

Received May 4, 1987; revised manuscript accepted September 22, 1987.